ELSEVIER

Biochimica et Biophysica Acta 1467 (2000) 113–123

BIOCHIMICA ET BIOPHYSICA ACTA
BBA

www.elsevier.com/locate/bba

Influence of the glycopeptidic moiety of mycobacterial glycopeptidolipids on their lateral organization in phospholipid monolayers

Isabelle Vergne [a,*], Bernard Desbat [b]

[a] *Institut de Pharmacologie et de Biologie Structurale, CNRS and Université Paul Sabatier, 31077 Toulouse Cedex, France*
[b] *Laboratoire de Spectroscopie Moléculaire et Cristalline, Université Bordeaux I, 33405 Talence, France*

Received 14 June 1999; received in revised form 23 March 2000; accepted 31 March 2000

Abstract

Glycopeptidolipids (GPLs) from the cell wall of opportunistic pathogenic mycobacteria are potential factors of pathogenicity which can interact with biological membranes. GPL suspensions uncouple oxidative phosphorylation of mitochondria and increase membrane permeability of liposomes. Heavily glycosylated GPLs are less active than lightly glycosylated ones. GPL–phospholipid interactions into preformed mixed films at the air–water interface were investigated in order to understand the permeabilization efficiency differences among GPLs. Polarization modulation infrared reflection absorption spectroscopy (PMIRRAS) was used to determine, in situ, the organization of GPL and of 1,2-di(perdeuteropalmitoyl)phosphatidylcholine (DPPC) molecules in mixed films. Compression isotherms of GPL alone or mixed with DPPC in various proportions showed that the less the GPL was glycosylated the higher its miscibility with DPPC. PMIRRAS studies indicated that low miscibility may result from large self-association of GPL molecules in β-sheet structures. Low glycosylated GPL molecules increased disorder of DPPC acyl chains. Based on these results, an explanatory model is proposed for membrane permeabilization. Increase of passive permeability may arise from disruption of phospholipid packing induced by GPL molecules. GPL segregation is proposed as the cause of low activity of GPL with high sugar content, by decreasing the number of GPL molecules interacting with phospholipids.

Keywords: Mycobacterium; Glycopeptidolipid–phospholipid interaction; Monolayer; Air–water interface; Fourier transform infrared spectroscopy; Beta-sheet

1. Introduction

Organisms belonging to the *Mycobacterium avium* complex are opportunistic pathogens which cause disseminated infection in patients with acquired immunity deficiency syndrome [1]. *M. avium* is an intracellular pathogen that can invade the macrophage and survive inside the phagosome by circumventing host cell defences [2,3].

Glycolipids from the cell wall of mycobacteria are potential factors involved in the pathogenesis [4,5]. Among them, glycopeptidolipids (GPLs) may participate in survival of *M. avium* in macrophages [6]. However, the mechanism of action of these molecules is still unknown, but as they are abundantly produced inside infected macrophages [7,8], and as

* Corresponding author. Present address: Department of Microbiology and Immunology, University of Michigan Medical School, 5641 Medical Science Building II, Ann Arbor, MI 48109-0620, USA. Fax: +1-734-764-3562;
E-mail: ivergne@umich.edu

0005-2736/00/$ – see front matter
PII: S0005-2736(00)00212-1

they are non-covalently linked to the outer portion of the cell envelope, we propose that they interact with host membranes and modify their organization and functional properties. Recent experiments support this hypothesis where GPL suspensions have been shown to uncouple oxidative phosphorylation of isolated rat liver mitochondria, to reduce mitochondrial transmembrane electrical potential ($\Delta\Psi$) and to increase passive permeability of liposomes [9,10]. It was thus postulated that GPL molecules inserted in the mitochondrial membranes make them more permeable to ions.

These molecules share the same peptidic backbone, acylated by a long chain C30 fatty acid, and differ by the number of saccharidic units present on the peptidic moiety (Fig. 1). The amplitude of the three observed effects was clearly related to the glycosylation level of GPLs, and the efficiency decreasing order was GPL1, GPL2, GPL3 and GPL5; GPL3 and GPL5 were barely active [10]. Surprisingly, the aglycone GPL (GPL0) was inactive on isolated mitochondria, as indicated in Section 3. A preliminary study was carried out in order to elucidate permeabilization efficiency differences [11], which indicated that GPL0 molecules in suspension were not able to insert from subphase into preformed phospholipid monolayers at the air–water interface, explaining the absence of membrane alteration by the absence of interaction. In the same work, GPL3 bearing three sugar residues appeared to insert in larger amounts than GPL1, although GPL1 was more active. From these results, it was postulated that the amplitude of the GPL effect likely depends on conformation and/or interaction of these molecules with phospholipids.

Fourier transform infrared spectroscopy (FT-IR) is a suitable technique to investigate peptide–phospholipid interactions [12]. Indeed, information on the conformation of phospholipids and peptides can be obtained simultaneously from spectra without addition of external probe. Unfortunately, few in situ studies of peptide–phospholipid films at the air–water interface have been achieved. The high absorption of the water vapor and the small number of molecules excited at the air–water interface require adapted FT-IR techniques. Gericke et al. managed to determine the conformation and orientation of L-α-dipalmitoylphosphatidylcholine (DPPC) acyl chains and of lung surfactant SP-C protein in mixed films using external infrared reflection–absorption spectroscopy (IRRAS) [13]. Recently, Blaudez et al. developed a new FT-IR technique based on differential reflectivity measurements by polarization modulation of the incident light (PMIRRAS) [14]. The conformation and orientation of the bee venom peptide melittin in a 1,2-dimyristoylphosphatidylcholine (DMPC) monolayer at the air–water interface have been determined as well as those of synthetic hemolytic peptides [15–17].

In order to gain more insight into the origin of the permeabilization efficiency difference among GPLs, the organization of GPLs in the presence or absence of phospholipids, and the ability of different GPLs to alter the surface properties and molecular order of phospholipids were investigated, using both compression isotherms and PMIRRAS. Since perturbations in phase transition can be used as a probe for intermolecular interactions, the present study was done using DPPC. A comparative study was performed with preformed mixed films at known GPL/phospholipid ratios, in order to overcome the problem resulting from differences of GPL insertion efficiencies.

2. Materials and methods

2.1. Materials

DPPC and 1,2-di(perdeuteropalmitoyl)phosphatidylcholine (DPPC-d_{62}) were purchased from Avanti Polar Lipids Inc. (Alabaster, AL, USA). The lipids were pure as determined by thin layer chromatography. Chloroform and methanol were distilled before use. Ultrapure water was obtained from a Millipore apparatus (MilliQ). The GPLs used were prepared from mycobacterial chloroform/methanol extracts as described previously [11]. Lipid solutions of defined composition used for monolayers were prepared in $CHCl_3/CH_3OH$ (8:2, v/v). Compounds for buffers were obtained from Merck (Darmstadt, Germany).

2.2. Tests of GPLs on mitochondria and liposomes

GPL0 activity on the oxidative phosphorylation of rat liver mitochondria was tested in conditions already published for GPL1–5 [9,10].

The absence of liposome fusion induced by GPLs was checked using a mixture of two types of liposomes (large unilamellar vesicles), labeled in their bilayer with phosphatidylethanolamine (PE)-NBD and PE-rhodamine and unlabeled, respectively, as in a previous publication [18]: fusion is accompanied by a mixing of the lipidic bilayers, which leads to an increase of NBD fluorescence.

2.3. Surface pressure–area measurements

Compression isotherms were performed using an equipment already described [19], with a Wilhelmy platinum plate to determine the surface pressure. The isotherms shown are the average of at least three assays obtained at 20°C, and were reproducible to within 1–4 nm^2/molecule. Monolayers were formed by carefully spreading 9–15 μl of lipid solution on a subphase with a starting surface area of 120 cm^2. The teflon trough was filled with a 5 mM phosphate buffer, 45 mM NaCl, pH 7.2 prepared with ultrapure water. After allowing solvent evaporation, monolayers were compressed at a rate of ca. 2.44 cm^2/min and pressure–area isotherms were recorded.

2.4. PMIRRAS apparatus

FT-IR spectra were recorded on a Nicolet 740 spectrometer equipped with a HgCdTe detector cooled to 77 K, by coaddition of 200 scans. A detailed description of the PMIRRAS set-up as well as the experimental procedure has already been published [20]. The infrared beam was polarized by a ZnSe grid and modulated by a ZnSe photoelastic modulator (PEM) between polarization (p) in the plane of incidence and polarization (s) perpendicular to this plane. For all experiments, the PEM was set to give half-wave retardation at 7 μm wavelength. The light beam was reflected at the air–water interface before being focused on the detector [21]. Optimal conditions for detection were obtained with an incidence angle of about 75° relative to the normal at the water surface.

The PMIRRAS signal can be expressed [20] as follows:

$$S = C\frac{(R_p - R_s)}{(R_p + R_s) + J_0(\Phi_0)(R_p - R_s)}J_2(\Phi_0) \quad (1)$$

where R_p and R_s are the polarized reflectivities, J_0 and J_2 are the zero and second-order Bessel functions, Φ_0 is the maximum dephasing given by the PEM, and C is a constant that depends on the electronic device.

Optically, in the mid-infrared range, water behaves as a dielectric substrate and therefore contributes to the PMIRRAS signal. In order to extract the weak absorption bands of the film and to get rid of the dependence on Bessel functions, the monolayer spectrum is ratioed by that of subphase buffer. In the normalized spectra, the direction of the bands versus the baseline is an indication of the orientation of the transition moment at the water surface and hence of that of the molecular groups themselves. For an incidence angle of 75° it has been determined [20] that an upward-oriented band indicates a transition moment occurring preferentially in the plane of the surface, whereas a downward-oriented band reveals an orientation preferentially perpendicular to the surface. For a given oscillator strength, bands associated with transition moments that are parallel to the surface are more intense compared to those perpendicular to the surface. When the angle Θ between the transition absorption moment and the surface normal is varied, absorption vanishes at $\Theta = 38°$. This value is determined by optical parameters, essentially by the refractive index of subphase.

2.5. FT-IR spectroscopy measurements

Absorbance spectra of GPL alone as bulk samples were obtained by transmission spectroscopy of organic solutions evaporated on a BaF_2 plate.

Monolayers were formed on a trough, with a surface area of 268 cm^2, placed in a water vapor-saturated enclosure at 20°C. The PMIRRAS spectra were acquired at a resolution of 4 cm^{-1} for GPL monolayers and DPPC-d_{62} monolayers and of 8 cm^{-1} for GPL/DPPC-d_{62} mixed films.

3. Results

3.1. Biological activities of GPLs

The effect of GPL1, 2, 3 and 5, but not that of GPL0, has already been tested on the oxidative phos-

GPL1:

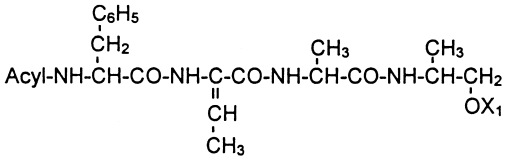

GPL0, GPL2, GPL3:

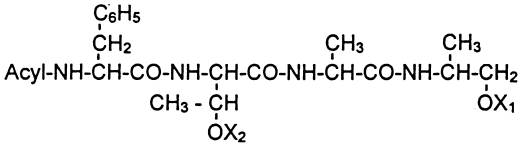

	GPL0	GPL1	GPL2	GPL3
X_1	H	3, 4-di-O-Me rhamnosyl or 2, 3, 4-tri-O-Me rhamnosyl	3, 4-di-O-Me rhamnosyl or 2, 3, 4-tri-O-Me rhamnosyl	3, 4-di-O-Me rhamnosyl (1->2) 3,4-di-O-Me rhamnosyl
X_2	H		6-deoxytalose	3-O-Me rhamnosyl

Acyl :

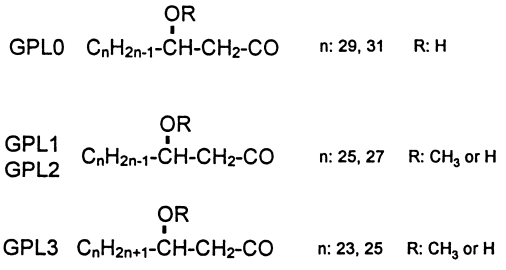

Fig. 1. Chemical structure of the GPLs and lipopeptide studied. The number following GPL corresponds to the number of carbohydrate residues linked to the peptide backbone.

phorylation of isolated rat liver mitochondria [9,10]. GPL0 was inactive (data not shown), even at the highest concentration used for the other GPLs (400 nmol GPL/mg of mitochondrial proteins).

As the increase of carboxyfluorescein release from liposomes induced by GPLs could result from solubilization and fusion of vesicles [9,10], the following control experiments were carried out. The absence of liposome fusion in the presence of GPLs was checked using a lipid mixing assay as in a previous publication [18] (data not shown). It was concluded that GPLs did not solubilize isolated mitochondria or liposomes because addition of GPLs did not induce a decrease of absorbance of mitochondrial and liposome suspensions (data not shown).

3.2. A macroscopic study of GPL/DPPC mixed monolayers

3.2.1. GPL1/DPPC and GPL0/DPPC

Fig. 2A,B shows typical compression isotherm curves of GPL0 and GPL1 alone or mixed with DPPC at given molar percentages. The x-axis corresponds to the molecular area of the mixture DPPC and GPL. The monolayer characteristics of the GPLs alone have been described elsewhere [11]. Briefly, the

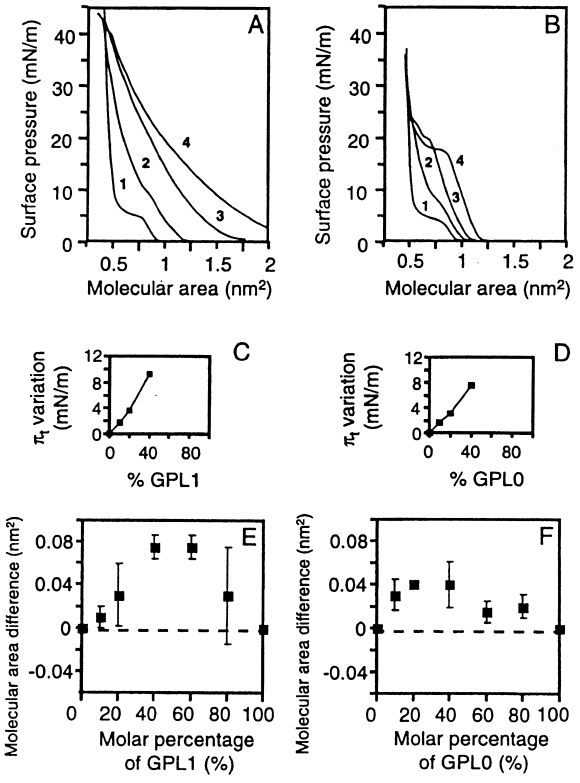

Fig. 2. Monolayers of GPL1, GPL0, DPPC and their mixtures. (A) GPL1; (B) GPL0. Surface pressure–area curves of spread monolayers of GPL, DPPC, and their mixtures on phosphate buffer. The molar percentage of GPL in monolayers was 0% (1), 20% (2), 60% (3), 100% (4). (C) GPL1; (D) GPL0. Variation of the DPPC transition pressure π_t as a function of monolayer composition. (E) GPL1; (F) GPL0. Plots of the difference in molecular area between the experimental π–A isotherms of mixed GPL/DPPC films and the corresponding theoretical isotherms as a function of GPL molar percentage at 25 mN/m. Dotted lines represent ideal mixing. For each GPL percentage, error bars were obtained from three isotherms.

GPL1 isotherm is monotonic and indicates high compressibility, the GPL0 isotherm shows a quasi-plateau at 18 mN/m, corresponding likely to a peptide transition between two conformations.

For mixed films, the surface pressure π_t at the beginning of the DPPC phase transition increased abruptly with the amount of GPL in the monolayer up to 40%, then no further DPPC phase transition was noted on the isotherm curves (Fig. 2C,D).

Fig. 2E,F displays the molecular area difference between the observed and the corresponding ideal isotherms for monolayers of GPL/DPPC mixtures as a function of the molar percentage of GPL at 25 mN/m (liquid-condensed phase). The molecular area difference showed positive deviations from the additivity rule, indicating that the mixed monolayer was expanded as compared to the individual components alone. The deviation from ideality is larger with GPL1 than with GPL0. We also noted a positive deviation at low pressures, negative deviations were only observed for GPL1/DPPC mixed monolayers at $\pi < 5$ mN/m (liquid-expanded phase) (data not shown). As a positive deviation can be observed for GPL1/DPPC (20/80) mixed monolayer at $\pi = 5$ mN/m (liquid-expanded phase) and at $\pi = 25$ mN/m (liquid-condensed phase), it seems that the negative deviation noted below 5 mN/m is due rather to surface pressure than to monolayer phase.

These results indicate both miscibility and non-ideality for the GPL1/DPPC and GPL0/DPPC systems. GPL1 and GPL0 molecules are miscible with DPPC in monolayers in all proportions as attested by the variations of the transition surface pressure and confirmed by the deviations of the molecular area versus percent GPL plots from the additivity rule. Thus, there are strong intermolecular interactions between GPL and DPPC molecules.

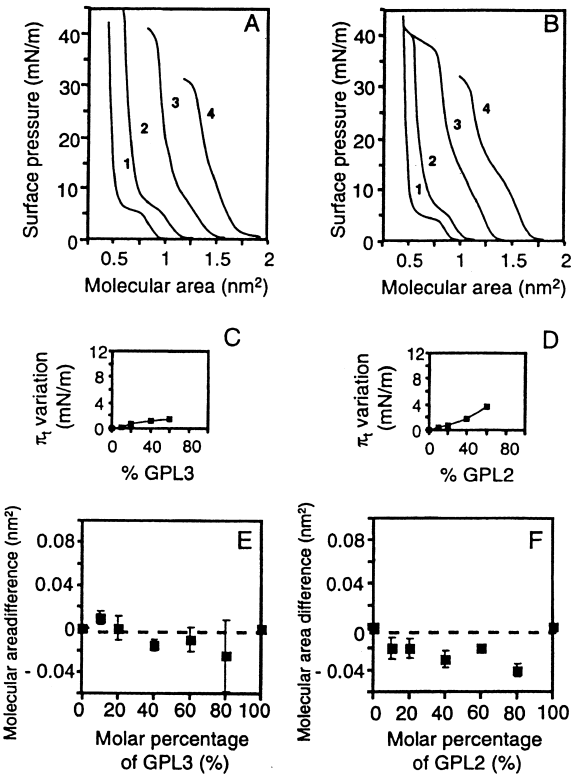

Fig. 3. Monolayers of GPL3, GPL2, DPPC and their mixtures. (A) GPL3; (B) GPL2. Surface pressure–area curves of spread monolayers of GPL, DPPC, and their mixtures on phosphate buffer. The molar percentage of GPL in monolayers was 0% (1), 20% (2), 60% (3), 100% (4). (C) GPL3; (D) GPL2. Variation of the DPPC transition pressure π_t as a function of monolayer composition. (E) GPL3; (F) GPL2. Plots of the difference in molecular area between the experimental π–A isotherms of mixed GPL/DPPC films and the corresponding theoretical isotherms as a function of GPL molar percentage at 25 mN/m. Dotted lines represent ideal mixing. For each GPL percentage, error bars were obtained from three isotherms.

3.2.2. GPL3/DPPC and GPL2/DPPC

Fig. 3A,B shows compression isotherms of binary mixtures of GPL3 or GPL2 with DPPC. For the mixed films, the transition surface pressure π_t increased slightly with the amount of GPL in the DPPC film (Fig. 3C,D).

Deviation of molecular area from the additivity rule was near zero at 25 mN/m (Fig. 3E) as well as at lower surface pressures (data not shown). In mixed monolayers of GPL3 with DPPC, deviations were in the range of the experimental error. The additive behavior of the average molecular areas for the mixtures of GPL3 with DPPC was consistent either with ideal mixing or with demixing of the GPL from the phospholipid. The slight increase of the transition surface pressure of DPPC with increasing amounts of GPL in the binary films rather suggested a large immiscibility.

The molecular area differences for mixtures of GPL2 and DPPC showed slight negative deviations from the additivity rule at 25 mN/m (Fig. 3F) and at lower surface pressures (data not shown) suggesting that the mixed monolayer was condensed as com-

pared to the individual components alone. These results indicate that GPL2 and DPPC are only partially miscible, and that GPL2 and GPL0 or GPL1 do not have identical interactions with DPPC.

3.3. A molecular study of GPL, DPPC and mixed monolayers

Compression curves of GPL–DPPC mixtures indicated that films with GPL0 or GPL1 were mostly expanded as compared to ideal films of DPPC and GPL. In contrast, films with GPL2 were slightly condensed. The non-ideal behavior of the phospholipid–GPL mixtures could be interpreted in terms of perturbations of the phospholipid hydrocarbon chain packing by GPL molecules, or conversely. In order to investigate the conformation of both GPL and phospholipid molecules alone or in mixed films, PMIRRAS was used.

3.3.1. GPL monolayers

FT-IR spectra of GPL monolayers at a surface pressure of 25 mN/m were recorded as well as those of solid anhydrous GPL for band assignment. C–H stretching vibrations of the acyl chain give rise to two bands in the 3100–2800 cm^{-1} region: antisymmetric and symmetric CH_2 bands with frequencies that are sensitive to the conformation and the *trans*/*gauche* ratio of the acyl chain segments. On GPL2 and GPL3 PMIRRAS spectra, these bands were absent, although they were detected on absorption spectra of solid anhydrous GPL (Fig. 4C,D). PMIRRAS band intensities depend on both transition moment orientation and molecular density of the monolayer. Otherwise, compression isotherms of one type of lipids showed that at 25 mN/m the area available per acyl chain of GPL2 and GPL3 is 6–7 times more important than the area of a DPPC acyl chain in all-*trans* conformation (Fig. 3A,B). This result indicates that the absence of CH_2 bands may result both from the low molecular density of GPL monolayers and from a disordered *gauche* conformation of the GPL acyl chain, due to the large area available to the chain. The GPL1 spectrum shows two broad bands at 2922 and 2854 cm^{-1} corresponding to antisymmetric and symmetric C–H stretching vibrations respectively (Fig. 4A). The GPL1 spectrum was repetitive and reproducible, so although

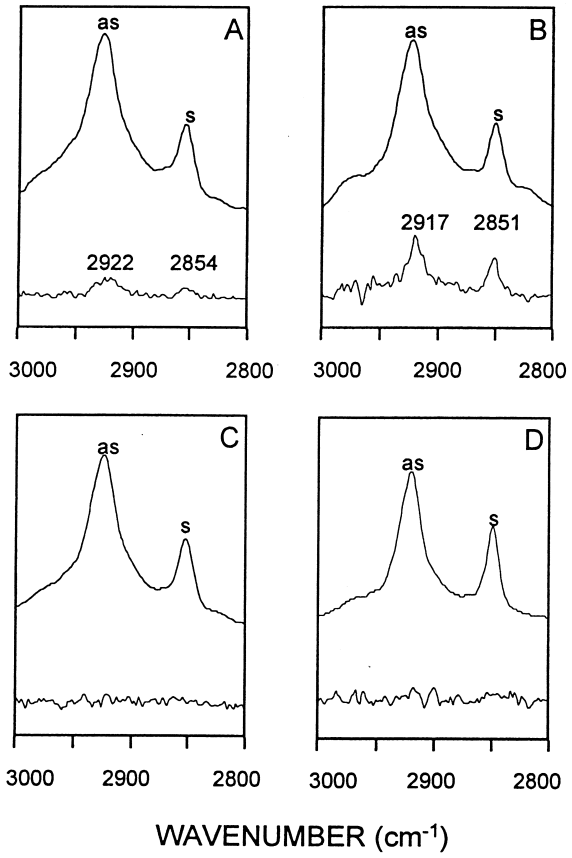

Fig. 4. CH stretching region of the FT-IR spectra of the GPL in different states. (A) GPL1; (B) GPL0; (C) GPL2; (D) GPL3. (Top spectrum) Absorption spectrum of GPL in solid state. (Bottom spectrum) In situ PMIRRAS spectrum of GPL film at 25 mN/m. as: antisymmetric; s: symmetric.

the signal-to-noise ratio is low, the assignment can be regarded as reliable. These results suggest a mostly *gauche* conformation of the acyl chain of GPL1 and are indicative of a highly disordered hydrocarbon chain [22]. The C–H stretching vibrations of the GPL0 acyl chain, on the other hand, were positioned at 2917 and 2851 cm^{-1} for antisymmetric and symmetric CH_2 bands respectively (Fig. 4B) and the bands were rather narrow indicating a high *trans*/*gauche* ratio along the acyl chains.

Fig. 5 shows the amide I and amide II band regions of absorption and PMIRRAS spectra. The broad dip at 1650 cm^{-1} is a feature of PMIRRAS spectra corresponding to different optical responses of the covered and uncovered water surface and to the spectral contribution of the water subphase [14,20]. The peptidic moiety gives rise mainly to a

strong band corresponding to C=O stretching (amide I) at a frequency which is conformation-sensitive, and to a weaker band corresponding to N–H bending (amide II). The GPL1 PMIRRAS spectrum shows a broad weak band at 1640 cm^{-1} (Fig. 5A); considering the size of the peptidic moiety, four amino acid residues and the width of the band, we propose that peptides form rather unordered structures. GPL0, and GPL2 and GPL3 exhibit an intense sharp peak at 1623 and at 1625 cm^{-1}, respectively (Fig. 5B–D) indicating the formation of β-sheets in GPL0, GPL2 and GPL3 monolayers [12,23,24]. These bands were also observed in the absorption spectra, therefore GPL0, GPL2 and GPL3 molecules were aggregated in β-sheets in the solid state. Because of the small size of the peptide (four amino acid residues), an intramolecular β-sheet can be excluded. We propose an intermolecular β-sheet arrangement of GPL0, GPL2 and GPL3 molecules in monolayers.

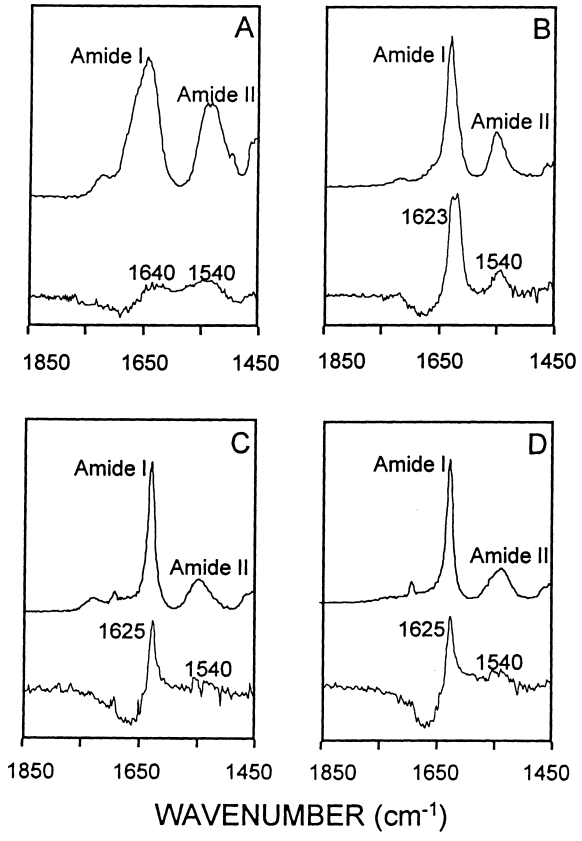

Fig. 5. Amide I and amide II band regions of the FT-IR spectra of GPL in different states. (A) GPL1; (B) GPL0; (C) GPL2; (D) GPL3. (Top spectrum) Absorption spectrum of GPL in solid state. (Bottom spectrum) In situ PMIRRAS spectrum of GPL film at 25 mN/m. Amide I: carbonyl stretching. Amide II: N–H bending.

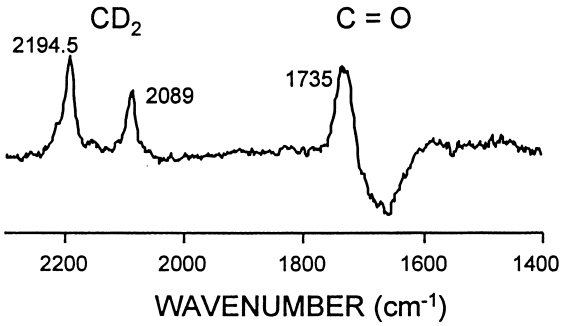

Fig. 6. The 2300–1400 cm^{-1} region of the DPPC-d_{62} monolayer PMIRRAS spectra. The film was compressed up to 25 mN/m. CD_2: C–D stretching vibration of the acyl chain. C=O: carbonyl stretching of ester bonds.

3.3.2. *DPPC-d_{62} film*

In order to follow conformational changes of phospholipid acyl chains in the presence of GPL, investigations were performed with DPPC-d_{62}. The isotopic substitution shifts the C–H stretching bands from high to low frequencies, thus, on mixed film spectra, the C–D bands can be detected independently of the GPL C–H bands and their frequencies can also account for the conformation of the acyl chains [25]. Fig. 6 shows the 2300–1400 cm^{-1} region of the PMIRRAS spectrum of a DPPC-d_{62} monolayer at 25 mN/m, in the liquid-condensed phase. The CD_2 stretching frequencies were observed at 2194.5 and 2089 cm^{-1} for antisymmetric and symmetric vibrations respectively. This result indicates mostly *trans* conformations along the acyl chains. The high intensity of these bands suggests a favorable orientation of the C–D bonds in the plane of the monolayer and ordered hydrocarbon chains [22,25]. Recently, Gericke et al. determined that the average acyl chain tilt angle from the surface normal was 26° for DPPC in a condensed phase at the air–water interface [13].

3.3.3. *Mixed films*

GPL–phospholipid interactions were monitored by forming monolayers of GPL/DPPC-d_{62} mixtures with 40% GPL at 25 mN/m. This ratio allowed detection of both the signals of phospholipid and those

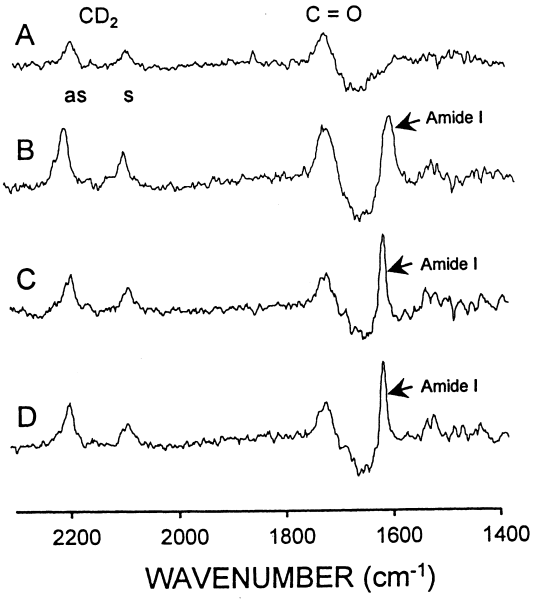

Fig. 7. The 2300–1400 cm^{-1} region of the mixed GPL/DPPC-d_{62} monolayer PMIRRAS spectra. The film was formed with 40% GPL and 60% DPPC-d_{62} and was compressed up to 25 mN/m. (A) GPL1; (B) GPL0; (C) GPL2; (D) GPL3. CD_2: C–D stretching vibration of phospholipid acyl chains. as: antisymmetric; s: symmetric; C=O: carbonyl stretching of phospholipid ester bonds. Amide I: carbonyl amide bond stretching.

of GPL molecules. The chosen surface pressure corresponded to a high molecular density, favoring a high signal-to-noise ratio. On GPL2 and GPL3 mixed film spectra (Fig. 7C,D), a sharp and intense amide I was noted at 1625 cm^{-1} and for GPL0 this band was positioned at 1620 cm^{-1} (Fig. 7B) suggesting that even when mixed with phospholipids, GPL molecules likely self-associate to form β-sheet structures. This self-assembly also occurred at low surface pressure, 5 mN/m (data not shown).

Data of CD_2 band analysis are reported in Table 1. Since the band area is not only sensitive to transition moment orientation but also to the surface molecular density, the integrated intensity was calculated for a constant surface density of DPPC-d_{62} molecules of one molecule per nm^2. In the presence of GPL1 (Fig. 7A), CD_2 stretching frequencies increased from 2194.6 to 2195.6 cm^{-1} for antisymmetric and from 2090.3 to 2094.5 cm^{-1} for symmetric vibrations. Integrated intensity decreased almost by a factor two, showing that the average transition moment tilt angle from the monolayer plane increased. GPL0 molecules altered the conformation of the phospholipid acyl chains in the same way, but the effects were not as strong as with GPL1. In contrast, a decrease of CD_2 frequencies and an increase of integrated intensity per molecule were noted with GPL3. Finally, GPL2 induced a decrease of the band area. These results suggest that GPL0, GPL2, and more intensely GPL1 molecules increased phospholipid acyl chain disorder either by disordering the orientational axis of the lipid or by increasing their number of *gauche* conformations. In contrast, GPL3 caused ordering of the phospholipid acyl chains.

4. Discussion

The main goal of the present study was to gain more insight into the interaction of mycobacterial GPLs with phospholipids in order to explain the different efficiencies among GPLs on membrane permeability. The organization of GPL molecules in phospholipid monolayers and the induced alteration of the phospholipid acyl chain conformation were investigated.

Table 1
Data of CD_2 stretching band analysis of DPPC-d_{62} and mixed film PMIRRAS spectrum at 25 mN/m

Film	Antisymmetric CD_2 stretching band		Symmetric CD_2 stretching band	
	Frequency (cm^{-1})	Integrated intensity[a]	Frequency (cm^{-1})	Integrated intensity[a]
DPPC-d_{62}	2194.6	2.5	2090.3	1.6
40% GPL1	2195.6	1.3	2094.5	0.8
40% GPL0	2195.1	2.2	2090.9	0.8
40% GPL2	2194.2	1.4	2090.7	1.1
40% GPL3	2193.8	3.5	2089.2	2.7

[a]Integrated intensities correspond to corrected integrated intensities calculated for surface density of DPPC-d_{62} of one molecule per nm^2.

Monolayers at the air–water interface appeared to be a convenient technique to carry out a comparative study, owing to the knowledge of the precise number of molecules at the interface. On the other hand, FT-IR was the most straightforward method to obtain conformational information on phospholipids and peptides without adding a probe. The PMIRRAS cumulated these advantages to allow in situ study of the conformation of peptides and lipids in monolayers at the air–water interface.

Infrared spectroscopy allows determination of the secondary structure of peptides or polypeptides. The peptidic moiety of the GPL molecule alone is too short to form a secondary structure, and in our experiments, bands were detected arising from self-association of GPLs, so GPL conformation analysis of isolated molecules cannot be achieved with this technique. Analysis of the amide band area indicated that GPL0, GPL2 and GPL3 formed β-sheets. This structure of the peptide may also be proposed from the amino acid sequence. Results from experiments by DeGrado and Lear showed that short amphiphilic peptides with a hydrophobic periodicity of 2 can form intermolecular antiparallel β-sheets at an apolar–water interface [26]. In addition, previous studies indicated that the critical peptide chain length for β-sheet formation is four amino acid residues [27]. The hydrophobic–hydrophilic alternation of amino acids in GPL3, GPL2 and GPL0 molecules results in an amphiphilic β-sheet with one side showing sugar residues or hydroxyl groups and the other exhibiting the aromatic rings, the methylene groups and the acyl chains. At the air–water interface, the hydrophilic moieties are likely exposed to the water phase while the hydrophobic moieties are in contact with air. A β-sheet structure was not observed in GPL1 monolayer, likely due to the presence of an α,β-dehydroamino acid residue which introduced significant conformational constraints in the peptidic backbone making the formation of intermolecular hydrogen bonds and pleating impossible [28].

Results obtained from PMIRRAS spectra together with those from mixed monolayer isotherms indicate that GPL3, GPL2 and GPL0 molecules tend to segregate from the DPPC phase. Indeed, GPL2 and GPL3 slightly increased the phase transition pressure of phospholipids, and the three GPLs gave rise to intermolecular β-sheet structures. Several experiments have reported that lateral phase separation of lipids depends on the nature of the head group and of the acyl chains [29,30]. It has been shown for mixtures of DPPC and gangliosides in bilayers that the greater the difference in the degree of unsaturation and chain length between the two lipid species, the higher their tendency to phase separation [30]. The same publication showed that for a given lipidic composition, this tendency was proportional to the number of sugar units on the ganglioside molecule. From another work [31], the hydrogen bonding network at the interface was found to be significant in miscibility properties of glycolipids and phospholipids. At first sight, from GPL structures (Fig. 1), lateral GPL segregation might result either from differences in the chemical composition of the acyl chain of the GPLs and the phospholipids (hydrocarbon chain length or unsaturation numbers), or from strong interactions between the glycopeptidic moieties of GPLs or from both. This study shows that GPL1 molecules can interact strongly with phospholipids, as seen from the increase in phase transition pressure of DPPC and from the expansion of mixed films although their acyl chain is twice as long as those of phospholipids. In addition, GPL1 molecules cannot self-associate in a β-structure. Finally, the self-association of GPL0, GPL2 and GPL3 molecules is observed at low and high surface pressures, i.e. with liquid-expanded phase and liquid-condensed phase respectively, indicating that GPL segregation is not related to the DPPC phase transition. These observations support the idea that the main driving force for GPL lateral segregation in GPL/DPPC monolayers is their ability to form intermolecular β-sheets. The non-glycosylated GPL (GPL0) changed the DPPC phase properties more intensely than GPL2 and GPL3, suggesting that sugars may favor GPL segregation by stabilizing aggregate clusters of GPL or by extending them by increasing the hydrogen bonding network among GPL molecules.

Analysis of the CD_2 bands of DPPC acyl chains showed that GPLs modify the phospholipid conformation in two ways: (i) the highly glycosylated GPL3 increased ordering in phospholipid chains, possibly by stabilization of the monolayer, through lipidic intermolecular hydrogen bonding, sugar residues forming hydrogen bonds with phospholipids in place of water molecules [32]; (ii) GPL0, GPL1 and

GPL2 increased the number of *gauche* conformers along the phospholipid acyl chains. For a same molar percentage of GPLs, GPL1 induced the highest alteration in the conformation of the phospholipid hydrocarbon part. These observations may be the outcome of a partial segregation of GPL molecules. Single monomeric or oligomeric GPLs cause a small local perturbation of lipid packing in the close vicinity of the GPL. The large segregation of GPLs diminishes the size of the contact interface with phospholipids, therefore the perturbation is weaker.

Control experiments indicate that the observed permeability increase does not result either from fusion or from solubilization of vesicles or of mitochondria. The present results show that the GPL molecules self-assemble in extended β-sheet structures or remain in monomeric or oligomeric form in the phospholipid monolayers. The question that arises is: which form induces an increase of membrane permeability? As GPL3 molecules are able to widely self-assemble, but do not induce carboxyfluorescein release from liposomes, in contrast to GPL1, we propose the following model: permeabilization would arise from interactions and shape mismatch between GPLs and phospholipid molecules which would result in an increase of organization defects in membranes. The permeabilization efficiency difference among GPLs would be due to segregation of highly glycosylated GPL molecules which decreases the number of GPL molecules interacting with phospholipids.

Previous results [11], together with those obtained in the present investigation, show that GPL0 and GPL3 have different behavior with regard to their interaction with membranes, which may explain their low activity. GPL0 molecules are miscible with phospholipids when they are presented in a mixed preformed film, but the absence of sugar units hinders their insertion from a GPL0 dispersion into phospholipid layers. In contrast, GPL3 molecules are able to insert efficiently into phospholipid layers but they segregate from the DPPC phase. In conclusion, it seems that the GPL with the highest efficiency to increase membrane passive permeability is one that has a sufficient sugar content to present a hydrophobic–hydrophilic balance that favors its insertion into membranes, but not enough sugar residues to form extensive β-structures or with a modified peptidic chain that prevent self-association in β-sheets, structures that exclude GPL molecules from phospholipid regions.

Acknowledgements

We thank Prof. G. Lanéelle and Dr. J.F. Tocanne for their constructive discussions and Prof. G. Lanéelle, Dr. J. Dufourcq and P. Winterton for the revision of the manuscript. This work was supported in part by Grant 920609 from the Institut National de la Santé et de la Recherche Médicale (France).

References

[1] C.R. Horsburgh, *Mycobacterium avium* complex infection in the acquired immunodeficiency syndrome, New Engl. J. Med. 324 (1991) 1332–1338.
[2] C. Frehel, C. de Chastellier, T. Lang, N. Rastogi, Evidence for inhibition of fusion of lysosomal and prelysososomal compartments with phagosomes in macrophages infected with pathogenic *Mycobacterium avium*, Infect. Immun. 52 (1986) 252–262.
[3] S. Sturgill-Koszycki, P.H. Schlesinger, P. Chakraborty, P.L. Haddix, H.L. Collins, A.K. Fok, R.D. Allen, S.L. Gluck, J. Heuser, D.G. Russell, Lack of acidification in *Mycobacterium* phagosomes produced by exclusion of the vesicular proton-ATPase, Science 263 (1994) 678–681.
[4] N. Rastogi, H.L. David, Mechanisms of pathogenicity in mycobacteria, Biochimie 70 (1988) 1101–1120.
[5] I. Vergne, M. Daffé, Interaction of mycobacterial glycolipids with host cells, Front. Biosci. 3 (1998) d865–876.
[6] W.W. Barrow, J.P. de Sousa, T.L. Davis, E.L. Wright, M. Bachelet, N. Rastogi, Immunomodulation of human peripheral blood mononuclear cell functions by defined lipid fractions of *Mycobacterium avium*, Infect. Immun. 61 (1993) 5286–5293.
[7] M.J. Tereletsky, W.W. Barrow, Postphagocytic detection of glycopeptidolipids associated with the superficial L1 layer of *Mycobacterium intracellulare*, Infect. Immun. 41 (1983) 1312–1321.
[8] S. Rulong, A.P. Aguas, P.P. da Silva, M.T. Silva, Intramacrophagic avium bacilli are coated by a multiple lamellar structure: freeze fracture analysis of infected mouse liver, Infect. Immun. 59 (1991) 3895–3902.
[9] A. Sut, S. Sirugue, S. Sixou, F. Lakhdar-Ghazal, J.F. Tocanne, G. Lanéelle, Mycobacteria glycolipids as potential pathogenicity effectors: alteration of model and natural membranes, Biochemistry 29 (1990) 8498–8502.
[10] L.M. Lopez-Marin, D. Quesada, F. Lakhdar-Ghazal, J.F. Tocanne, G. Lanéelle, Interactions of mycobacterial glyco-

peptidolipids with membranes: influence of carbohydrate on induced alterations, Biochemistry 33 (1994) 7056–7061.
[11] I. Vergne, M. Prats, J.F. Tocanne, G. Lanéelle, Mycobacterial glycopeptidolipid interactions with membranes: a monolayer study, FEBS Lett. 375 (1995) 254–258.
[12] J.L.R. Arrondo, F.M. Goñi, Infrared spectroscopic studies of lipid–protein interactions in membranes, in: A. Watts (Ed.), Protein–Lipid Interactions, Elsevier, Amsterdam, 1993, pp. 321–349.
[13] A. Gericke, C.R. Flach, R. Mendelsohn, Structure and orientation of lung surfactant SP-C and L-α-dipalmitoylphosphatidylcholine in aqueous monolayers, Biophys. J. 73 (1997) 492–499.
[14] D. Blaudez, T. Buffeteau, J.C. Cornut, B. Desbat, N. Escafre, M. Pézolet, J.M. Turlet, Polarization-modulated FT-IR spectroscopy of spread monolayer at the air/water interface, Appl. Spectrosc. 47 (1993) 869–874.
[15] I. Cornut, B. Desbat, J.M. Turlet, J. Dufourcq, In situ study by polarization modulated fourier transform infrared spectroscopy of the structure and orientation of lipids and amphipathic peptides at the air-water interface, Biophys. J. 70 (1996) 305–312.
[16] S. Castano, B. Desbat, I. Cornut, P. Méléard, J. Dufourcq, α-helix to β-sheet transition within the Leu_iLys_j (i = 2j) series of lytic amphipathic peptides by decreasing their size, Lett. Peptide Sci. 4 (1997) 1–6.
[17] S. Castano, B. Desbat, M. Laguerre, J. Dufourcq, Structure, orientation and affinity for interfaces and lipids of ideally amphipathic lytic L_iK_j (i = 2j) peptides, Biochim. Biophys. Acta 1416 (1999) 176–194.
[18] J. Gonzalez-Christen, I. Vergne, R. Sußmuth, S. Sidobre, M. Prats, J.-F. Tocanne, G. Lanéelle, Adjuvant lipopeptide interaction with model membranes, Biochim. Biophys. Acta 1368 (1998) 97–107.
[19] K. Nicolay, A.M. Sautereau, J.F. Tocanne, R. Brasseur, P. Huart, J.M. Ruysschaert, B. de Kruijff, A comparative model membrane study on structural effects of membrane-active positively charged anti-tumor drugs, Biochim. Biophys. Acta 940 (1988) 197–208.
[20] D. Blaudez, T. Buffeteau, J.C. Cornut, B. Desbat, N. Escafre, M. Pézolet, J.M. Turlet, Polarization modulation FT-IR spectroscopy at the air-water interface, Thin Solid Films 242 (1994) 146–150.
[21] D. Blaudez, J.M. Turlet, J. Dufourcq, D. Bard, T. Buffeteau, B. Desbat, Investigations at the air-water interface using polarization modulation IR spectroscopy, J. Chem. Soc. Faraday Trans. 92 (1996) 525–530.
[22] M.L. Mitchell, R.A. Dluhy, In situ FT-IR investigation of phospholipid monolayer phase transitions at the air-water interface, J. Am. Chem. Soc. 110 (1988) 712–718.
[23] C.R. Flach, J.W. Brauner, J.W. Taylor, R.C. Baldwin, R. Mendelsohn, External reflexion FT-IR of peptide monolayer films in situ at the air/water interface: experimental design, spectra-structure correlations, and effects of hydrogen-deuterium exchange, Biophys. J. 67 (1994) 402–410.
[24] P.I. Haris, D. Chapman, The conformational analysis of peptides using fourier transform IR spectroscopy, Biopolymers 37 (1995) 251–263.
[25] F.R. Rana, A.J. Mautone, R.A. Dluhy, Surface chemistry of binary mixtures of phospholipids in monolayers. Infrared studies of surface composition at varying surface pressures in a pulmonary surfactant model system, Biochemistry 32 (1993) 3169–3177.
[26] W.F. DeGrado, J.D. Lear, Induction of peptide conformation at apolar/water interfaces. 1. A study with model peptides of defined hydrophobic periodicity, J. Am. Chem. Soc. 107 (1985) 7684–7689.
[27] M. Narita, Y. Tomotake, S. Isokawa, T. Matsuzawa, T. Miyauchi, Syntheses and properties of resin-bound oligopeptides. 2. Infrared spectroscopic conformational analysis of cross-linked polystyrene resin bound oligoleucines in the swollen state, Macromolecules 17 (1984) 1903–1906.
[28] T.P. Singh, P. Kaur, Conformation and design of peptides with α,β-dehydro-amino acid residues, Prog. Biophys. Mol. Biol. 66 (1996) 141–165.
[29] E.J. Shimshick, H.M. McConnell, Lateral phase separation in phospholipid membranes, Biochemistry 12 (1973) 2351–2360.
[30] M. Masserini, P. Palestini, E. Freire, Influence of glycolipid oligosaccharide and long-chain base composition on the thermotropic properties of dipalmitoylphosphatidylcholine large unilamellar vesicles containing gangliosides, Biochemistry 28 (1989) 5029–5034.
[31] R.D. Koynova, H.L. Kuttenreich, B.G. Tenchov, H.J. Hinz, Influence of head-group interactions on the miscibility of synthetic, stereochemically pure glycolipids and phospholipids, Biochemistry 27 (1988) 4612–4619.
[32] J.M. Boggs, Lipid intermolecular hydrogen bonding: influence on structural organization and membrane function, Biochim. Biophys. Acta 906 (1987) 353–404.